

5-1-2020

Understanding Protein-Nanoparticle Interactions Using Nuclear Magnetic Resonance

Sarah Claxton
Mississippi State University

Follow this and additional works at: <https://scholarsjunction.msstate.edu/honorsthesis>

Recommended Citation

Claxton, Sarah, "Understanding Protein-Nanoparticle Interactions Using Nuclear Magnetic Resonance" (2020). *Honors Theses*. 71.
<https://scholarsjunction.msstate.edu/honorsthesis/71>

This Honors Thesis is brought to you for free and open access by the Undergraduate Research at Scholars Junction. It has been accepted for inclusion in Honors Theses by an authorized administrator of Scholars Junction. For more information, please contact scholcomm@msstate.libanswers.com.

UNDERSTANDING PROTEIN-NANOPARTICLE INTERACTIONS USING NUCLEAR MAGNETIC RESONANCE

By

Sarah E. Claxton

UNDERSTANDING PROTEIN-NANOPARTICLE INTERACTIONS USING NUCLEAR MAGNETIC RESONANCE

I. Abstract

The study of gold nanoparticles (AuNP) is an increasingly prominent research field that covers a wide range of techniques, including biosensing, drug and gene therapy, and bioimaging. When exposed to biological fluids, AuNPs will interact with proteins in solution, and these proteins will compete to bind to the surface of the nanoparticle. While it still remains difficult to predict the competitive binding of proteins to the nanoparticle surface, the advent of applicable data could be instrumental in aiding research scientists' approaches to targeting nanoparticles to specific cells in the body and functionalizing them for particular applications. Nuclear magnetic resonance (NMR) is one approach for studying this biological interaction, and in this work, 2D ^1H - ^{15}N HSQC methods were used to visualize the protein interaction thermodynamics and kinetics with nanoparticles. A ^1H - ^{15}N HSQC technique was used to quantify AuNP binding versus time for a mixture of GB3 and Ubiquitin (Ubq), two small model proteins. In addition, Amidase (AM) and R2ab, two larger protein domains of autolysin protein from *Staphylococcus epidermidis*, were used to further understand the AuNP-protein interactions. The proteins were incubated for an hour with AuNPs and sampled at several differing concentrations; an external standard was used to quantify absolute binding to the AuNPs. Our results and subsequent model for GB3 and Ubq suggest that competitive binding is not strictly kinetically controlled but potentially thermodynamically controlled. Conversely, competition between AM and R2ab for

the nanoparticle surface seems to be kinetically controlled due to an agreement between observed values and a model under strict kinetic control. Both sets of results suggest a mechanism by which the surface of the AuNP may change over time and may be an important consideration in the design of nanoparticle-based therapeutics.

II. Introduction

Nanoparticles have been of pronounced scientific interest because of their numerous biological applications, including drug and gene delivery, chemo- and phototherapy, biosensing, and bioimaging.^{1-2,6} Because of their simple synthesis, well-defined surface chemistry, and non-toxicity, nanoparticles of various materials can withstand surface modifications to offer toxicological and pharmacological advantages.¹⁻⁴ Some of these various nanomaterials include silica, noble metals, metal oxides, and polymers; however, in recent years gold nanoparticles (AuNPs) have been particularly attractive in drug-delivery systems as well as other biological systems.¹ Upon the introduction of AuNPs to a biological mixture, proteins in solution will spontaneously bind to the surface of the nanoparticle to form a protein corona. This corona, however, is not a fixed coating but can change over time due to several factors, including protein concentrations, binding affinity, and the size and charge.^{2,4-6} Understanding this unique interaction of protein-AuNP adsorption can provide insight into how specific proteins and nanoparticles can be used in biologically relevant systems.

In previous studies, GB3 and Ubiquitin were used as model proteins to investigate the electrostatic interactions taking place at the nanoparticle surface.⁷ These proteins are well characterized and are easily isotopically labeled for NMR experiments. In early studies, the 1D NMR data suggested that competition at the AuNP surface largely favors proteins with a higher

net charge.⁷ Additionally, the protein corona changes in various pH environments over time and also plays a role in the binding affinity of proteins.⁷ The same NMR-based protein competition approach can be applied to other protein mixtures, such as biofilm forming proteins.

Biofilms are surface-associated multicellular communities that are created by bacterial microbes.¹⁴ The structural integrity of biofilms is highly dependent on its extracellular matrix comprised of proteins, polysaccharides, and nucleic acids.¹⁶ Biofilms confer resistance to antibiotics and host immune responses.¹⁴⁻¹⁶ *Staphylococcus epidermidis* (*S. epidermidis*) autolysin E (AtlE) biofilm proteins are of notable interest because of this organism's association with infections of implanted medical devices.¹⁶ *S. epidermidis* AtlE contains a multidomain structure. The amidase domain has been previously shown to interact with polystyrene surfaces through hydrophobic and van der Waal's interactions.¹⁷ Investigating how biofilm forming proteins interact with the AuNP surface independently and in competition will give further insight into biofilm development on various nanoparticle surfaces, since the AtlE protein is thought to be involved in the initial attachment to surfaces in some medical contexts.

In this study, we explore how solution concentration influences protein competition on the AuNP surface. Competition between GB3 and Ubq serves as a testbed for a model incorporating both kinetic and thermodynamic control. Then, once established, the model can be used to understand how biofilm-forming proteins interact with AuNPs. During the protein competition studies, the GB3-Ubq data suggested imperfect packing on the surface while the biofilm-forming protein mixture behaved similarly to our theoretical values.

III. Materials and Methods

A. Citrate Stabilized AuNP Preparation

Gold(III) chloride trihydrate and sodium citrate dihydrate were acquired from Sigma Aldrich. The citric acid reduction method was used to synthesize 15-nm gold nanoparticles.¹¹ Once a mixture of 99 mL MQ water and 1 mL of HAuCl_4 was brought to a boil, approximately 2 mL of a 1% sodium citrate solution was immediately added to the gold solution. After continuing to boil for 20 minutes, the gold nanoparticle mixture was allowed to cool for several hours. The nanoparticle size and shape were assessed by UV-visible spectroscopy and transmission electron microscopy.¹¹ The maximum absorbance was observed at 520 nm, as expected for this 15 nm diameter spheres.¹¹

B. Protein Mixtures with AuNPs

Individual protein solutions (20 μM) were prepared in 20 mM phosphate buffer at pH 7 and with 10% D_2O as the lock solvent. To determine the amount of bound protein to the surface of the nanoparticle, a 20 mM ^{15}N Urea external standard was used during the NMR analysis. Each 20 μM protein solution was mixed with 20, 40, 60, and 80 nM AuNP solutions and incubated for approximately an hour before recording the NMR spectra.

Solutions containing two proteins, GB3-Ubq or R2ab-AM, were prepared as a dilution series with a total protein concentration of 50 μM . While one protein increased in concentration, the other protein's concentration decreased over the course of 7 increments between 0 μM and 50 μM . The protein mixtures for GB3 and Ubq were added to 80 nM AuNP solution and incubated for an hour before recording NMR spectra. For the R2ab and AM experiments, the protein mixtures were added to 60 nM AuNP solution instead of 80 nM AuNP solution.

C. NMR Analysis

^1H - ^{15}N heteronuclear single-quantum coherence (HSQC) NMR spectra were collected on a 600 MHz Bruker Avance III cryoprobe-equipped instrument at 298 K as described previously.^{7,11} An acquisition time of 300 ms (512 complex points) was used for the single protein AuNP titrations and the protein competition experiments. The total experiment time for each spectrum was 1 hr and 22 min.

The ^1H - ^{15}N HSQC spectra were processed using NMRPipe.¹⁸ The peak assignments for both the GB3 and Ubq experiments and the R2ab and AM experiments were obtained from previous studies. The assignments used for GB3 in this study were Y3, N8, G9, T17, V21, D22, G38, D47, K50, and E56. The assignments used for Ubq in this study were K6, T12, V17, D21, K29, Q31, Q49, S57, L67, and H68. The assignments used for AM in this study were K307, R335, E338, T344, G358, T370, A385, T466, T477, and R487. The assignments used for R2ab in this study were L699, N704, A712, Y722, I732, D767, G809, N834, S837, and G838.

IV. Results and Discussion

A. 1D vs. 2D NMR Experiments

In previous studies, 1D NMR titrations were used for determining the binding capacity of a protein adsorbed to the gold nanoparticle surface in addition to monitoring the kinetics of two proteins competing for the AuNP surface.^{7,11} These studies successfully observed the binding of the model proteins on the surface by isotopically labeling GB3 (^{13}C) and Ubq (^{15}N). The ^{13}C labeled residues of the protein correspond to the aliphatic proton region (0-4 ppm), while the ^{15}N labeled residues correspond to the amide proton region (6-11 ppm) on a 1D NMR spectrum.^{7,11} As a result of increasing AuNP concentration in solution, the protein peak intensity decreases

without altering or shifting the peak. The signal decrease in the presence of nanoparticles is quantifiably related to the amount of bound protein on the surface and is calculated by scaling the peaks to the internal standard of TMSP as a reference.^{7,11} The binding capacity for GB3 and Ubq at pH 7 are 177 and 156 molecules per NP, respectively.¹¹ To monitor both proteins simultaneously binding to the nanoparticle surface, each protein must have a different isotope label.

In our study, all proteins were labeled with ¹⁵N to continue monitoring the backbone amide region of the proteins, and a 2D NMR method was applied. The second dimension was advantageous because the peaks produced in the spectra corresponded to individual residues unique to each protein. A ¹⁵N Urea external standard was used as a reference to scale the peak intensities and quantify the amount of protein bound to the surface of the AuNP. Because the chemical shift pattern does not overlap with either of the protein's peaks, Urea was chosen as an effective reference.

Before starting the competition experiments, GB3 and Ubq were individually titrated against varying concentrations of AuNPs to determine the binding capacity using 2D HSQC. The binding capacity for each protein was determined and compared to the 1D NMR values to verify the use of 2D NMR for our analysis (Table 1). GB3 and Ubq were calculated to have binding capacities of 180 and 156, respectively. The binding capacity of each protein was graphed against the concentration of nanoparticles, and the linear projection confirmed that the AuNPs were saturated (Figure 1C).

Once the proteins interacting with the nanoparticle surface were analyzed independently using 2D NMR, the two proteins were mixed over 7 increments to observe competition on the

AuNP. Ten residues for each protein were selected to monitor because they lack spectral overlap and appear to behave similarly in the presence and absence of nanoparticles (Figure 1A and 1B).

Table 1 Protein-AuNP Binding Capacities

Binding Capacities			
Protein	Predicted Values	1D NMR Values	2D NMR Values
GB3	199 ²⁰	177	180
Ubq	155 ²⁰	156	156
Amidase	85	-	92
R2ab	71	68	77

Predicted values were calculated based on protein structure and radius of the nanoparticles.

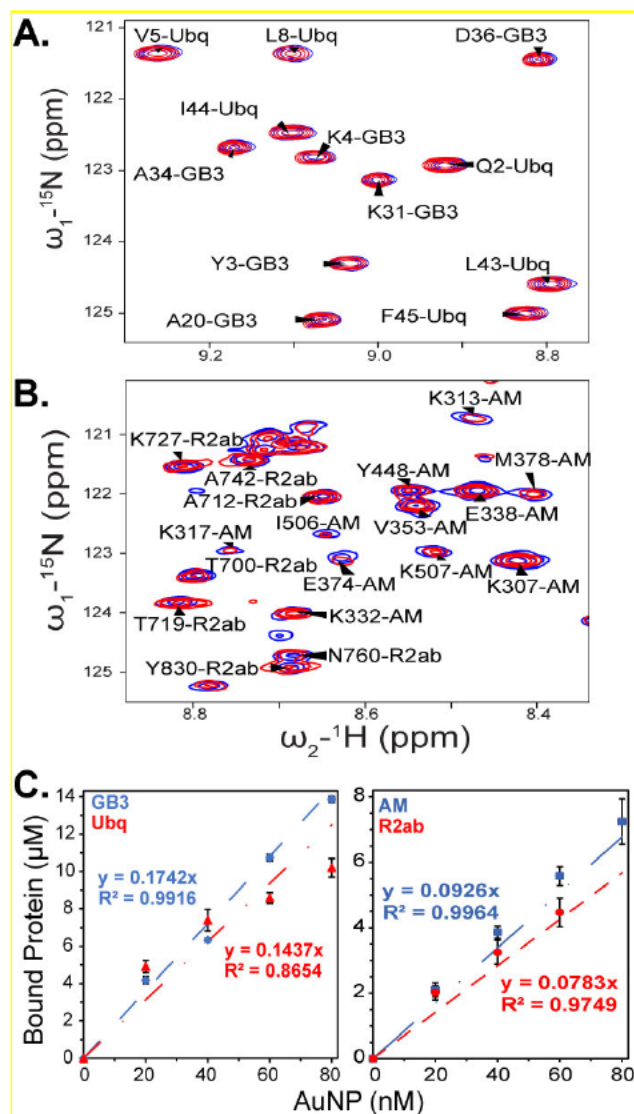


Figure 1 Protein Binding Capacities on AuNP Surface

Backbone amide ^1H - ^{15}N heteronuclear single-quantum coherence (HSQC) experiment used to quantify proteins isotopically labeled the same in solution. (A) 25 μM ^{15}N -labeled GB3 and 25 μM ^{15}N -labeled Ubq mixed with 80 nM AuNP and (B) 25 μM ^{15}N -labeled AM and 25 μM ^{15}N -labeled R2ab mixed with 60 nM AuNP. The peak intensities were measured for the mixed protein solutions in the presence (red spectra) and absence (blue spectra) of AuNPs. (C) The binding capacity for each protein is determined using the HSQC experiment by plotting the bound protein concentration versus various AuNP concentrations. 20 μM of each protein was mixed with 0, 20, 40, 60, and 80 nM AuNP to identify how many molecules of protein are bound to the NP surface. The observed concentrations for GB3 (blue diamonds), Ubq (red triangles), AM (blue squares), and R2ab (red circles) are plotted against their expected values.

B. Protein Competition and Model

Upon introduction of a protein mixture to nanoparticle solution, the protein corona will spontaneously begin to form due to the binding affinity of proteins to the AuNP surface.^{2,4-6} The use of GB3 and Ubq as model proteins in this protein competition study investigates the kinetic and thermodynamic nature of the AuNP-protein interaction. Because little is known about the kinetics of this interaction, we designed a model to investigate the formation of the protein corona during competition.

A kinetically controlled competition suggests a theoretical binding pattern in which the proteins behave similarly with the AuNP surface due to their size and shape.⁷ While Ubq is slightly larger than GB3 (76 vs 56 residues), both GB3 and Ubq have roughly similar sizes and geometric shapes, as indicated by the similar binding capacities. However, if one protein interacted more favorably to the surface, that more protein molecules would bind to the surface relative to the weaker binding protein.⁷ Our model begins with a schematic illustration of the protein competition for the AuNP surface (Figure 2A). Protein A (blue) represents GB3 and protein B (red) represents Ubq. The rate at which proteins bind to the surface and competition occurs in our model is dependent on two reaction terms. The k_1 term corresponds to both proteins interacting with the soft corona, the outer layer of the AuNP shell. While this is a reversible process, k_1 for GB3 and Ubq must be larger than their respective k_{-1} terms because binding is observed. The hardening rate at which proteins are tightly bound to the surface in the hard corona¹⁹ is represented by the k_2 term. This reaction is not reversible because the protein is fixed once bound to the citrate coated AuNP surface.

This simple kinetic model was designed to monitor the competition between proteins when the fraction in solution for protein A ranged from 0-1 and the fraction of protein B exhibited the

opposite (1-0). By altering the binding (k_1 and k_{-1}) and hardening (k_2) rates, the model depicts whether the protein mixture will behave in a kinetically controlled competition (Figure 2B). For example, if k_{-1} is faster than k_2 , an equilibrium will be established in the soft corona, and binding will be thermodynamically controlled by the more favorable binding protein. On the other hand, if k_2 is faster than k_{-1} , and if both proteins have similar affinity for the surface, binding will be kinetically controlled. This is because the protein with the higher concentration will collide stochastically with the nanoparticle surface more frequently, leading to a successful hard corona transition. The system is under-determined, and many combinations of rate constants can produce the same behavior. The modeled data falls near the theoretical values (dashed lines) for the majority of the cases; however, the modeled data deviates significantly from the theoretical when the binding ratio and hardening rates change over time. When both the binding ratio and hardening rate are low, protein B is favored in the competition. As the value continues to change across the diagonal and on the right side of the matrix, the data moves closer to the theoretical lines and eventually favors protein A.

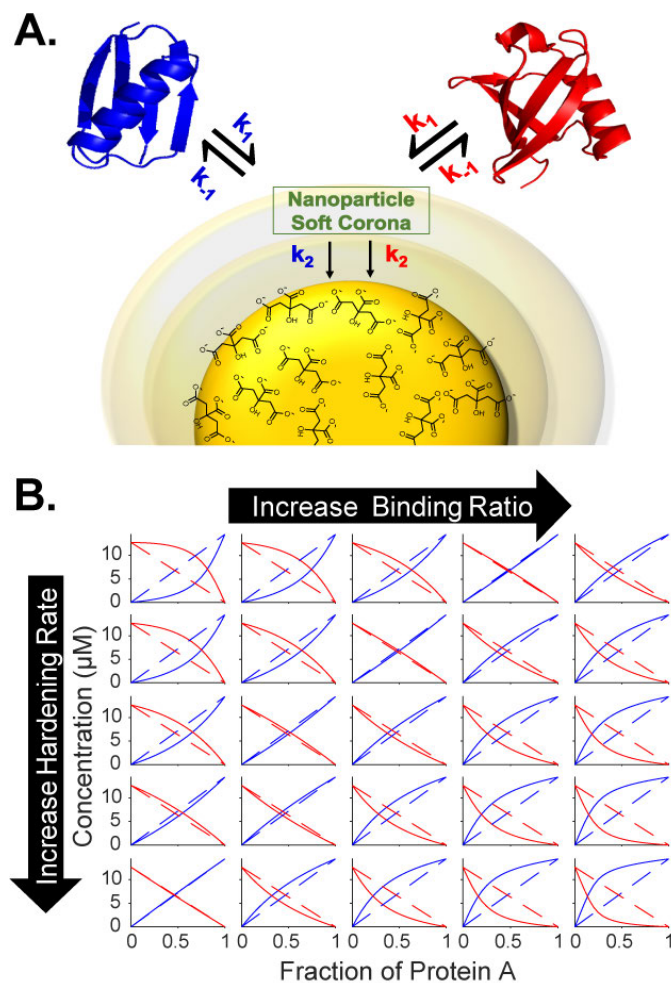


Figure 2 Protein Competition Model onto the AuNP Surface

(A) A schematic diagram of two proteins kinetically competing onto the AuNP surface. Protein A (GB3) and Protein B (Ubq) are in the free environment competing for the surface resulting a reversible reaction (k_1 and k_{-1}). The first initial contact with the AuNP surface is in the soft corona, or the outermost layer of the AuNP. Once the soft corona and free environment reach equilibrium, in a forward reaction (k_2), the proteins will form a monolayer in the hard corona, or the innermost layer of the AuNP where the binding occurs. (B) A 5x5 grid that represents how kinetics influence the shape of the modeled data. Each graph is a representation of a series of matrices that have varying kinetic rates. Moving left and right in the figure represents how increasing the binding ratio, how quickly the proteins reach equilibrium, influences the shape of the model data. Moving up and down in the figure represents how increasing the hardening rate, how quickly a monolayer on the surface forms, also influences the shape of the model data. As observed in the graphs, if one protein is above the theoretical line the other protein is below the theoretical and will eventually approach the theoretical line.

Based on our model, it is expected that protein competition favors certain proteins of higher concentration in solution. This expectation from the kinetic model was not observed in the experimental data for the GB3-Ubq competition. The data differs from the theoretical values significantly in that the curve representing GB3 binding remains below the dashed line and the Ubq curve has a sigmoidal shape (Figure 3). The results of this competition experiment suggest that the simple kinetic model is not sufficient to completely explain this specific interaction. In the matrix of graphs depicting the kinetically controlled reaction of the proteins with the surface of the nanoparticle, a sigmoidal shape for protein B was not observed. This deviation from the theoretical data might be due to protein-protein interactions or protein deformation on the surface causing imperfect packing. Additionally, consideration of other factors affecting the binding and adsorption process between proteins and the AuNP surface could significantly alter the theoretical binding projection.

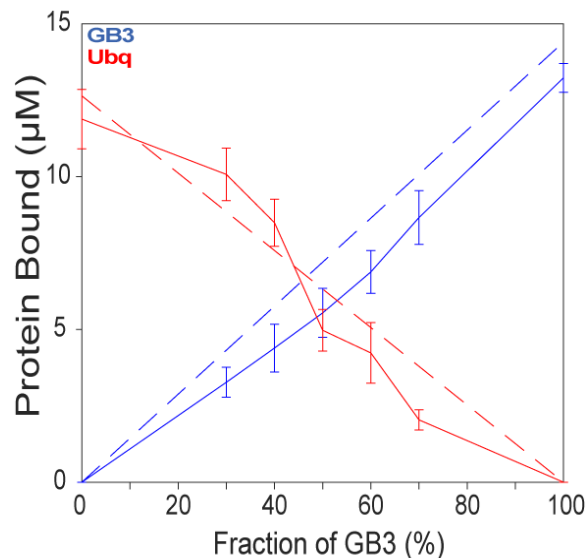


Figure 3 Model Proteins Competition

GB3 (blue) and Ubq (red) competition onto the AuNP Surface (80 nM). The protein bound (μM) vs. fraction of GB3 (%) determines the behavior of the competition. There are 7 points per solid line that represents the fraction of GB3 (%) used in each mixture - 0, 30, 40, 50, 60, 70, and 100 % fraction of GB3. The blue and red dashed lines represent the theoretical value (binding capacity). The binding capacity for each protein interacting with 80 nM AuNP were 14.4 (GB3) and 12.6 (Ubq) molecules per NP. The error bars represent the 95% confidence interval (CI) – 95% CI = standard error of the mean * Z-value. The Z-value for 95% CI is 1.96.

C. Biofilm Forming Protein Competition

Our work with *S. epidermidis* AltE involved the amidase catalytic domain and R2ab proteins (Figure 4). The same theoretical adsorption behavior, as detailed above, was expected for this competition experiment. R2ab and AM differ in size and shape; therefore, slight deviations from the theoretical pattern were expected. However, data from the protein competition revealed that R2ab and AM interacted similarly to the theoretical values (Figure 5). Because of this and the information from our simple kinetic model, it is believed that R2ab-AM competition for the AuNP surface is strictly kinetically controlled.

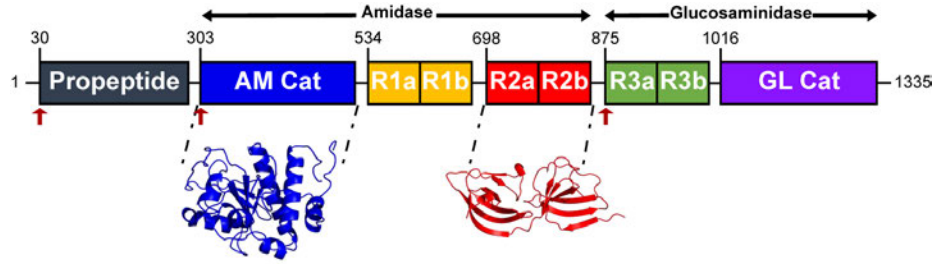


Figure 4 Structure of *S. epidermidis* AltE biofilm forming proteins

The two domains that comprise AltE are emphasized at the top: Amidase and Glucosaminidase. The Amidase domain contains the amidase catalytic domain and three half-open β -barrel Rab proteins. In this study, the amidase catalytic domain (AM) and R2ab are the biofilm proteins of interest.

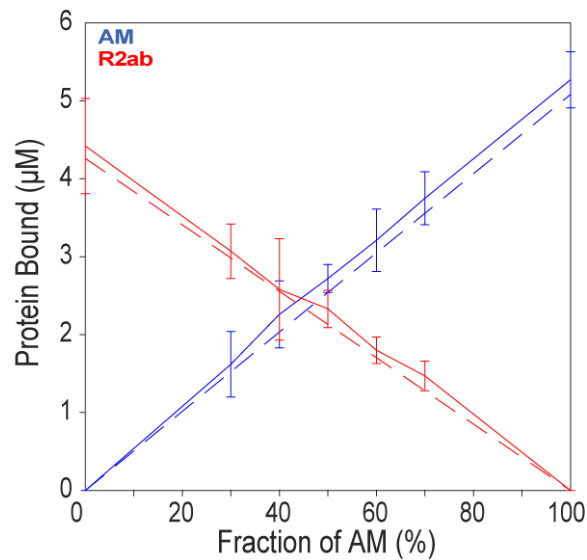


Figure 5 Biofilm Forming Proteins Competition

AM (blue) and R2ab (red) competition onto the AuNP Surface (60 nM). The protein bound (μM) vs. fraction of AM (%) determines the behavior of the competition. There are 7 points per solid line that represents the fraction of AM (%) used in each mixture. These points are 0, 30, 40, 50, 60, 70, and 100 % fraction of AM. The blue and red dashed lines represent the theoretical value (binding capacity). The binding capacity for each protein interacting with 60 nM AuNP were 5.08 (AM) and 4.42 (R2ab) molecules per NP. The error bars represent the 95% confidence interval (CI) – 95% CI = standard error of the mean * Z-value. The Z-value for 95% CI is 1.96.

V. Conclusion

In our study, a 2D NMR approach was used to quantify the protein competition interactions for the GB3-Ubq mixture and the R2ab-AM mixture. All proteins were isotopically labeled (^{15}N), and the second dimension allowed for sufficient peak separation and ability to monitor independent backbone residues for each protein. A model was introduced whereby protein adsorption could potentially be under a mixture of thermodynamic and kinetic control, and we adapted this model to visualize experiments where proteins were allowed to compete for the same nanoparticle surface. While both GB3-Ubq and R2ab-AM fell fairly close to the straight lines indicating strict kinetic control, the results from the GB3-Ubq competition showed some deviation from the shapes predicted from the model under any combination of thermodynamic and kinetic control. The data for GB3-Ubq protein competition might suggest imperfect packing on the AuNP surface or protein-protein interactions. In contrast, the R2ab-AM competition behaved similarly to the theoretical values and seems to be kinetically controlled based on our model.

VI. Acknowledgments

I thank Dr. Fitzkee and his entire lab, including post-docs, graduate students, and undergraduate students. I specifically appreciate Becca Hill and her continued efforts on this project.

VII. References

1. Biju, V. Chemical Modifications and Bioconjugate Reactions of Nanomaterials for Sensing, Imaging, Drug Delivery and Therapy. *Chemical Society Reviews* 2014, 43 (3), 744-764.
2. Aili, D.; Gryko, P.; Sepulveda, B.; Dick, J. A.; Kirby, N.; Heenan, R.; Baltzer, L.; Liedberg, B.; Ryan, M. P.; Stevens, M. M. Polypeptide Folding-Mediated Tuning of the Optical and Structural Properties of Gold Nanoparticle Assemblies. *Nano Lett* **2011**, 11 (12), 5564-5573.
3. Ginzburg, A. L.; Truong, L.; Tanguay, R. L.; Hutchison, J. E. Synergistic Toxicity Produced by Mixtures of Biocompatible Gold Nanoparticles and Widely Used Surfactants. *ACS Nano*. 2018, 12 (6), 5312-5322.
4. Lin, W.; Insley, T.; Tuttle, M. D.; Zhu, L.; Berthold, D. A.; Král, P.; Rienstra, C. M.; Murphy, C. J. Control of Protein Orientation on Gold Nanoparticles. *The Journal of Physical Chemistry C* 2015, 119 (36), 21035-21043.
5. Casals, E.; Pfaller, T.; Duschl, A.; Oostingh, G. J.; Punties, V. Time Evolution of the Nanoparticle Protein Corona. *ACS Nano* 2010, 4 (7), 3623-3632.
6. Gagner, J. E.; Qian, X.; Lopez, M. M.; Dordick, J. S.; Siegel, R. W. Effect of Gold Nanoparticle Structure on the Conformation and Function of Adsorbed Proteins. *Biomaterials*. 2012, 33 (33), 8503-8516.
7. Wang, A.; Perera, Y. R.; Davidson, M. B.; Fitzkee, N. C. Electrostatic Interactions and Protein Competition Reveal a Dynamic Surface in Gold Nanoparticle-Protein Adsorption. *The Journal of Physical Chemistry C* 2016, 120 (42), 24231-24239.
8. Freeman RG, Hommer MB, Grabar KC, Jackson MA, Natan MJ. Ag-Clad Au Nanoparticles: Novel Aggregation, Optical, and Surface-Enhanced Raman Scattering Properties. *J. Phys. Chem.* 1996; 100:718.
9. Link S, El-Sayed MA. Size and Temperature Dependence of the Plasmon Absorption of Colloidal Gold Nanoparticles. *J. Phys. Chem. B.* 1999; 103:4212.
10. Jain PK, Lee KS, El-Sayed IH, El-Sayed MA. Calculated Absorption and Scattering Properties of Gold Nanoparticles of Different Size, Shape, and Composition: Applications in Biological Imaging and Biomedicine. *J. Phys. Chem. B.* 2006; 110:7238. [PubMed: 16599493]
11. Wang A, Vangala K, Vo T, Zhang D, Fitzkee NC. A Three-Step Model for Protein-Gold Nanoparticle Adsorption. *J. Phys. Chem. C.* 2014; 118:8134-8142.
12. Vilanova, O.; Mittag, J. J.; Kelly, P. M.; Milani, S.; Dawson, K. A.; Rädler, J. O.; Franzese, G. Understanding the Kinetics of Protein-Nanoparticle Corona Formation. *ACS Nano*. 2016, 10 (12), 10842-10850.
13. Milani, S.; Baldelli Bombelli, F.; Pitek, A. S.; Dawson, K. A.; Rädler, J. Reversible Versus Irreversible Binding of Transferrin to Polystyrene Nanoparticles: Soft and Hard Corona. *ACS Nano*. 2012, 6 (3), 2532-2541.

14. Branda, S. S.; Vik, Å.; Friedman, L.; Kolter, R. Biofilms: The Matrix Revisited. *Trends in Microbiology* 2005, 13 (1), 20-26.
15. Heilmann, C.; Hussain, M.; Peters, G.; Götz, F. Evidence for Autolysin-Mediated Primary Attachment of *Staphylococcus Epidermidis* to a Polystyrene Surface. *Molecular Microbiology* 1997, 24 (5), 1013-1024.
16. O'Gara, J. P.; Humphreys, H. *Staphylococcus Epidermidis* Biofilms: Importance and Implications. *Journal of Medical Microbiology* 2001, 50 (7), 582-587.
17. Biswas, R.; Voggu, L.; Simon, U. K.; Hentschel, P.; Thumm, G.; Götz, F. Activity of the Major *Staphylococcal* Autolysin Atl. *FEMS Microbiology Letters* 2006, 259 (2), 260-268.
18. Delaglio, F.; Grzesiek, S.; Vuister, G.; Zhu, G.; Pfeifer, J.; Bax, A. Nmrpipe: A Multidimensional Spectral Processing System Based on Unix Pipes. 1995; Vol. 6, p 277-293.
19. Vilanova, O.; Mittag, J. J.; Kelly, P. M.; Milani, S.; Dawson, K. A.; Rädler, J. O.; Franzese, G. Understanding the Kinetics of Protein–Nanoparticle Corona Formation. *ACS Nano*. 2016, 10 (12), 10842-10850.
20. Assfalg, M.; Ragona, L.; Pagano, K.; D'Onofrio, M.; Zanzoni, S.; Tomaselli, S.; Molinari, H. The Study of Transient Protein–Nanoparticle Interactions by Solution NMR Spectroscopy. *Biochimica et Biophysica Acta (BBA) - Proteins and Proteomics* 2016, 1864 (1), 102-114.